

Experimental Study of the Reaction $e^+e^- \rightarrow K_S K_L$ in the Energy Range $\sqrt{s} = 1.04 \div 1.38$ GeV.

M. N. Achasov,^{1,2} K. I. Beloborodov,^{1,2,*} A. V. Berdyugin,¹ A. V. Bozhenok,^{1,2}
D. A. Bukin,¹ T. V. Dimova,¹ V. P. Druzhinin,^{1,2} V. B. Golubev,^{1,2}
I. A. Koop,^{1,2} A. A. Korol,¹ S. V. Koshuba,¹ A. P. Lysenko,¹
A. V. Otboev,¹ E. V. Pakhtusova,¹ S. I. Serednyakov,^{1,2} Yu. M. Shatunov,^{1,2}
V. A. Sidorov,¹ Z. K. Silagadze,^{1,2} A. N. Skrinsky,¹ and A. V. Vasiliev^{1,2}

¹*Budker Institute of Nuclear Physics, Novosibirsk, 630090, Russia*

²*Novosibirsk State University, Novosibirsk, 630090, Russia*

(Dated: June 1, 2006)

We present a measurement of the $e^+e^- \rightarrow K_S K_L$ cross section in the energy range $\sqrt{s} = 1.04 \div 1.38$ GeV. For the energy $\sqrt{s} \geq 1.2$ GeV the cross section exceeds vector meson dominance model predictions with only $\rho(770)$, $\omega(783)$, and $\phi(1020)$ mesons taken into account. Measured cross section agrees well with previous measurements.

PACS numbers: 13.66.Bc 14.40.Aq 13.40.Gp 12.40.Vv

I. INTRODUCTION

The spectroscopy of light-quark vector mesons is still far from completion. It is mostly because not all the processes are measured with sufficient accuracy. One of the sources of new information on vector meson spectroscopy is a process $e^+e^- \rightarrow K_S K_L$, into which contribute isoscalar $\omega(783)$, $\phi(1020)$, and isovector $\rho(770)$ resonances as well as their higher mass excitations. Accurate measurement of the $e^+e^- \rightarrow K_S K_L$ cross section is also important because it is a part of the total cross section of the electron-positron annihilation into hadrons, which enters into calculations of the hadronic vacuum polarization contribution to the anomalous magnetic moment of the muon and running electromagnetic coupling constant at Z -boson mass $\alpha_{\text{em}}(M_Z)$.

*Electronic address: K.I.Beloborodov@inp.nsk.su

At present the $e^+e^- \rightarrow K_S K_L$ cross section is measured with an accuracy of few per cent only in the narrow energy interval around $\phi(1020)$ resonance [1, 2]. First measurements of this reaction at higher energy were conducted with DM1 [3] and OLYA [4] detectors. The DM1 measurement at DCI collider covers the energy range $\sqrt{s} = 1.40 \div 2.18$ GeV with a total integrated luminosity of 1.4 pb^{-1} . The OLYA measurements in the energy range $\sqrt{s} = 1.06 \div 1.40$ GeV were carried out at VEPP-2M collider with the total integrated luminosity of 0.7 pb^{-1} . In both experiments significant excess of the $e^+e^- \rightarrow K_S K_L$ cross section over vector meson dominance (VMD) model was observed. The latest measurement of the $e^+e^- \rightarrow K_S K_L$ cross section was done by CMD-2 detector [5] in the energy range \sqrt{s} from 1.05 up to 1.40 GeV.

In this work the measurement of the $e^+e^- \rightarrow K_S K_L$ cross section in the energy range from 1.04 up to 1.38 GeV is reported. The experiment was carried out with SND detector at VEPP-2M e^+e^- collider. The analysis is based on the total integrated luminosity of 9.1 pb^{-1} .

II. DETECTOR AND EXPERIMENT

The SND detector [6] operated at VEPP-2M e^+e^- collider complex from 1995 up to 2000. It was designed as a universal detector for the studies of the decays of ρ , ω , ϕ resonances as well as the processes of e^+e^- annihilation into hadrons in the energy range $\sqrt{s} = 0.40 \div 1.40$ GeV.

The main part of the SND detector is a three-layer scintillation electromagnetic calorimeter consisted of 1632 counters with NaI(Tl) crystals. The total thickness of the calorimeter for the particles originating from the detector center is 13.4 radiation lengths. The energy resolution of the calorimeter for photons is $\sigma_E/E = 4.2\% / \sqrt[4]{E(\text{GeV})}$. The angular resolution is equal to $\sigma_\phi, \sigma_\theta \simeq 1.5^\circ$. The solid angle coverage is 90% of 4π . The charged particle tracks are measured by ten-layer drift chamber system located inside the calorimeter.

In this analysis the data collected in the experimental runs of 1997 and 1999 are used. In 1997 two scans of the energy range from 0.96 up to 1.38 GeV with an energy step of 10 MeV and the total integrated luminosity of 6 pb^{-1} were performed. The year 1999 scan was done in the energy range from 1.02 to 1.34 GeV with a step of 10 MeV and a total integrated luminosity of 3.1 pb^{-1} . In this analysis the points with $\sqrt{s} \geq 1.04$ GeV were considered.

III. DATA ANALYSIS

The process

$$e^+e^- \rightarrow K_S K_L \quad (1)$$

was studied in the decay mode $K_S \rightarrow \pi^0 \pi^0 \rightarrow 4\gamma$. The K_L mesons, due to their large decay length, which is much larger than the detector radius, and large nuclear interaction length in the NaI(Tl) (~ 0.35 m), do not produce any signal in the detector in a significant part of events. Nuclear interaction of the K_L meson or its decay inside the detector produce energy deposits in the calorimeter counters, which are interpreted by the event reconstruction program as one or more photons. In both cases appearance of charged particles in the tracking system is improbable. Thus, for the analysis of the process (1) only the events with no charged particle tracks in the drift chamber are considered. The main background processes for the process under study are the following:

$$e^+e^- \rightarrow \omega \pi^0 \rightarrow \pi^0 \pi^0 \gamma, \quad (2)$$

$$e^+e^- \rightarrow \phi(\gamma) \rightarrow \eta \gamma(\gamma) \rightarrow 3\pi^0 \gamma(\gamma), \quad (3)$$

$$e^+e^- \rightarrow \phi \gamma \rightarrow K_S K_L \gamma \quad (4)$$

The process (4) is a radiative “return” to the ϕ resonance due to emission of photon(s) by initial particles. These photons are mostly emitted at small angle with respect to the beam direction and thus are not detected. The process (3) is a sum of the processes $e^+e^- \rightarrow \eta \gamma$ and $e^+e^- \rightarrow \eta \gamma \gamma$ with additional photon emitted by initial particles. Other background sources considered in the analysis are beam background and cosmic particles.

Initial event selection is based on the following criteria:

- $N_\gamma \geq 4$, where N_γ is a number of reconstructed photons;
- $N_c = 0$, where N_c is a number of reconstructed charged particles;
- events with a cosmic particle track reconstructed in the calorimeter are rejected. The track in the calorimeter is a group of calorimeter crystal hits positioned along a common straight line.

The last requirement reduces the number of selected events by more than a factor of two, almost completely rejecting the background from cosmic particles.

The events satisfying these criteria are kinematically fitted in the hypothesis of $K_S \rightarrow \pi^0\pi^0 \rightarrow 4\gamma$ decay. The kinematic fitting procedure searches for the combination of two photon pairs from π^0 decays. The invariant mass of found π^0 's is constrained to the mass of K_S meson. There is no constraints on K_S energy. In a multi-photon events for all four-photon combinations corresponding χ^2 are calculated, and the combination with a minimum χ^2 ($\chi_{K_S \rightarrow 2\pi^0}^2$) is chosen. The $\chi_{K_S \rightarrow 2\pi^0}^2$ distributions for different selection criteria are shown in Figs. 1 and 2. For further analysis the events with $\chi_{K_S \rightarrow 2\pi^0}^2 < 25$ are selected. The following additional selection criteria are applied to these events:

1. $\zeta_i < 0$ ($i = 1..4$), where ζ_i is a “quality” parameter of a reconstructed photon equal to $-\log L$, where L is a likelihood function value of a hypothesis that observed transverse energy distribution in the cluster of hit calorimeter crystals corresponds to one isolated photon [7]. This parameter provides separation between events with isolated photon showers and those with merged showers or clusters from K_L -meson nuclear interactions or decays.
2. $36^\circ < \theta_i < 144^\circ$, where θ_i is a polar angle of the photon included in the reconstructed K_S meson with respect to the beam direction. This criterion rejects significant part of the beam background.
3. $400 < M_{rec} < 550$ MeV, where M_{rec} is a recoil mass of the reconstructed K_S meson:

$$M_{rec} = \sqrt{\sqrt{s}(\sqrt{s} - 2E_{K_S}) + M_{K_S}^2}, \quad (5)$$

\sqrt{s} — total energy in the center-of-mass frame, E_{K_S} — the energy of the reconstructed K_S meson, M_{K_S} is a K_S -meson mass. This requirement suppresses background from the process (4).

4. $\chi_{\pi^0\pi^0\gamma}^2 > 60$, where $\chi_{\pi^0\pi^0\gamma}^2$ is a χ^2 of the kinematic fit in the $e^+e^- \rightarrow \pi^0\pi^0\gamma$ hypothesis. This criterion is applied to events with $N_\gamma \geq 5$ to suppress the background from the process (2).

The total number of events satisfying all criteria described above in the full energy range is equal to 1998, of which 585 events are in the region $\sqrt{s} \geq 1.1$ GeV.

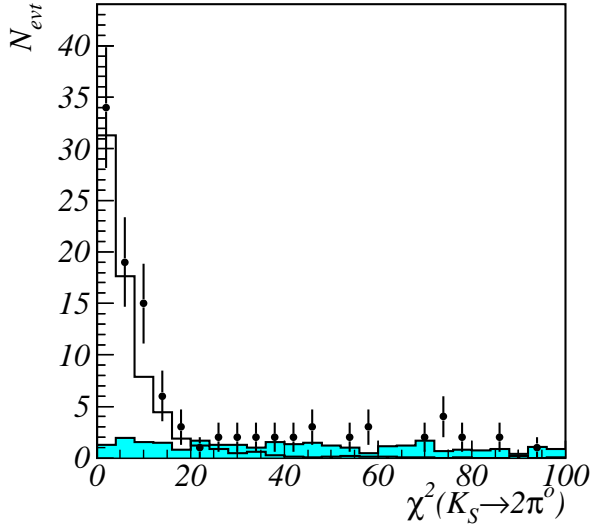


FIG. 1: The $\chi^2_{K_S \rightarrow 2\pi^0}$ distribution for the events with $\sqrt{s} > 1.2$ GeV, $N_\gamma < 7$, and $E_{tot} \geq 0.5 \cdot \sqrt{s}$. Dots with error bars — data, line — simulation of the process (1), shaded histogram — simulation for the process (2).

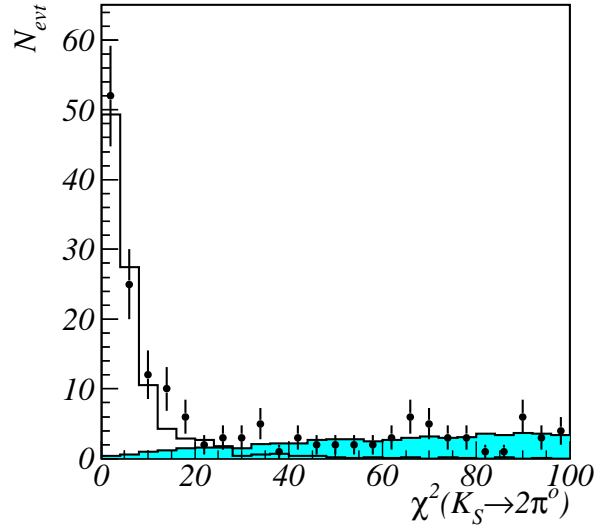


FIG. 2: The $\chi^2_{K_S \rightarrow 2\pi^0}$ distribution for the events with $\sqrt{s} > 1.12$ GeV and $E_{tot} < 0.5 \cdot \sqrt{s}$. Dots with error bars — data, line — simulation for the process (1), shaded histogram — experimental distribution for the beam background.

The number of background events of the process $e^+e^- \rightarrow \omega\pi^0$ was estimated from Monte Carlo simulation. The cross section of the process (2) was taken from the paper [8], in which was also shown that the simulation of the multi-photon events in SND detector agrees with experiment within 5%. We checked the accuracy of the $e^+e^- \rightarrow \omega\pi^0$ background estimation using experimental data. The error estimation is based on approximation of the $\chi^2_{K_S \rightarrow 2\pi^0}$ distribution (Fig. 1) for events with $\sqrt{s} > 1.2$ GeV, $N_\gamma < 7$ and $E_{tot} \geq 0.5 \cdot \sqrt{s}$, where E_{tot} is a total energy deposition in the calorimeter. These requirements effectively suppress contributions from all background processes except (2). The distribution is approximated by a sum of the process under study and (2), obtained by simulation and shown in Fig. 1. This experimental estimation agrees within statistical accuracy with that obtained by simulation. The total number of events of this background process in the full energy range with all selection criteria applied is $N_{\omega\pi^0} = 11.3 \pm 0.3 \pm 2.3$.

The number of background events of the process $e^+e^- \rightarrow \eta\gamma(\gamma)$ is also estimated by simulation. The events of this process satisfying all selection criteria are dominated by radiative return to ϕ resonance: $e^+e^- \rightarrow \phi\gamma$, $\phi \rightarrow \eta\gamma$, in which the photons emitted by

initial particles are not detected. The accuracy of the estimation of this process contribution is $\approx 3\%$. It is determined by the accuracy of the $e^+e^- \rightarrow \eta\gamma$ cross section measurements near the ϕ resonance ($\approx 2\%$), and the accuracy of the $e^+e^- \rightarrow \eta\gamma\gamma$ cross section calculation (1%). The total number of the background events of this process is $21.2 \pm 0.2 \pm 1.1$.

For the estimation of the beam background the $\chi_{K_S \rightarrow 2\pi^0}^2$ distribution shown in Fig. 2 was used. The dots with error bars show the experimental $\chi_{K_S \rightarrow 2\pi^0}^2$ distribution for the energy range $\sqrt{s} > 1.12$ GeV with additional selection criterion $E_{tot} < 0.5\sqrt{s}$, which rejects events of all background processes except beam background. The shaded histogram shows the experimental distribution for the beam background events, for which the selection criteria inverse of 1 and 2 were used. The total number of the beam background events is estimated as $N_b = 30 \pm 3 \pm 5$.

The contribution of the $e^+e^- \rightarrow K_S K_L \gamma$ events strongly depends on the beam energy. For the energy region close to ϕ resonance the photon energy E_γ is small in comparison with the total energy \sqrt{s} making this process virtually indistinguishable from $e^+e^- \rightarrow K_S K_L$. With the increase of collision energy the photon energy grows and the kinematics of the processes (1) and (4) becomes more distinct. The recoil mass spectra against reconstructed K_S meson are shown in Fig. 3 for four energy intervals. The peak with a mean value close to the K^0 -meson mass is due to the reaction $e^+e^- \rightarrow K_S K_L$, the rest corresponds to the process $e^+e^- \rightarrow K_S K_L \gamma$. Good separation between these processes can be achieved at energies above 1.2 GeV. At lower energy the processes (1) and (4) cannot be separated. To solve this problem the approximation of the cross section was carried out with the detection efficiency as a function of both \sqrt{s} and the energy of the photon emitted by initial particles.

The distribution of the number of selected events, background from $e^+e^- \rightarrow \omega\pi^0$ and $e^+e^- \rightarrow \eta\gamma(\gamma)$ as function of energy with the beam background subtracted is presented in Table I.

IV. DETECTION EFFICIENCY

The detection efficiency for the process under study was determined using Monte Carlo simulation. The simulation takes into account photon emission by initial particles [9, 10], permitting us to take into account the dependence of the detection efficiency $\varepsilon(\sqrt{s}, z)$ on energy \sqrt{s} and $z = \frac{E_\gamma}{\sqrt{s}}$, the fraction of energy carried away by the photon emitted by

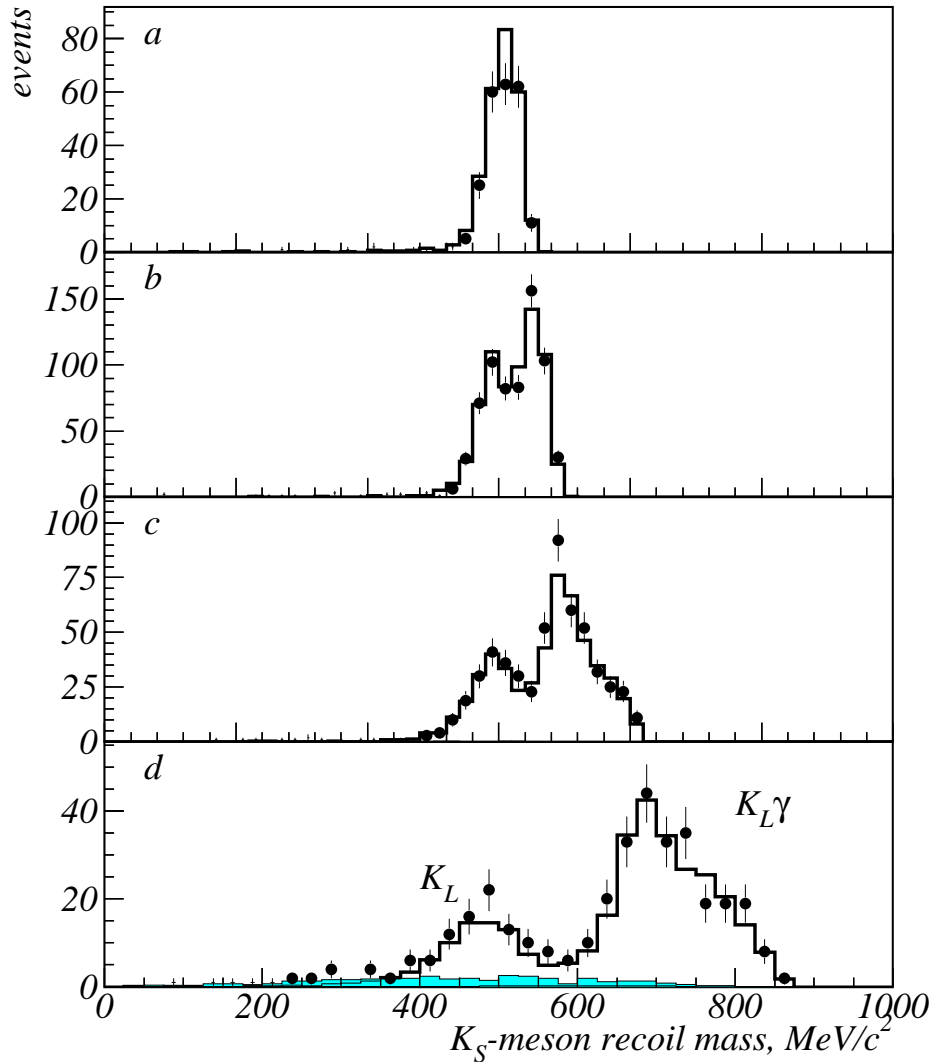


FIG. 3: The recoil mass spectra against reconstructed K_S meson in four energy intervals: a) $\sqrt{s} = 1.04 - 1.05$ GeV, b) $\sqrt{s} = 1.06 - 1.09$ GeV, c) $\sqrt{s} = 1.10 - 1.20$ GeV, d) $\sqrt{s} = 1.20 - 1.38$ GeV. The spectrum is for events, satisfying additional selection criteria: $N_\gamma < 7$ $E_{tot} \geq 0.5\sqrt{s}$. The shaded histogram shows estimated $e^+e^- \rightarrow \omega\pi^0$ background.

initial particle. The energy dependence of the detection efficiency for the process (1) with $E_\gamma < 10$ MeV is shown in Fig. 4. The decrease of the efficiency at large \sqrt{s} is caused by degradation of resolution in kinematically fitted K_S -meson recoil mass for energies, which are far from $K_S K_L$ production threshold. Fig. 5 shows the detection efficiency dependence on E_γ for several energy points.

The correction for the detection efficiency, which takes into account the difference in

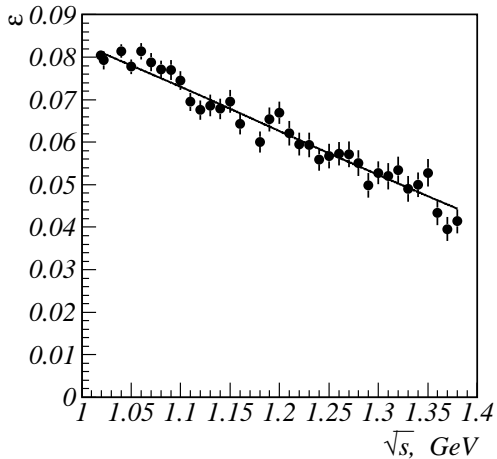


FIG. 4: Detection efficiency for the process (1) as a function of energy for the events with the energy of the photon emitted by initial particles $E_\gamma < 10$ MeV.

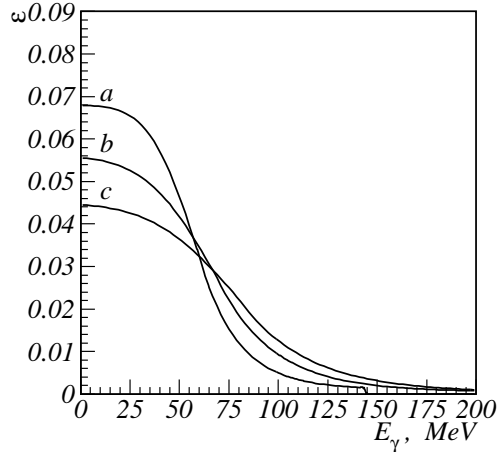


FIG. 5: Detection efficiency for the process (1) as a function of the energy E_γ of the photon emitted by initial particles for three different energies: a — $\sqrt{s} = 1.15$ GeV, b — $\sqrt{s} = 1.27$ GeV, c — $\sqrt{s} = 1.38$ GeV.

detector response between data and simulation was estimated using events from the ϕ -resonance region, where the process (1) can be separated with a negligible background without constraints on $\chi^2_{K_S \rightarrow 2\pi^0}$ and ζ_i . The following selection criteria were applied: $N_\gamma = 5$, $E_{\gamma_5} > 100$ MeV, $\angle(\mathbf{n}_{K_S}, \mathbf{n}_{\gamma_5}) > 130^\circ$, where E_{γ_5} is an energy of the photon not included in the reconstructed K_S meson, $\angle(\mathbf{n}_{K_S}, \mathbf{n}_{\gamma_5})$ is an angle between directions of the reconstructed K_S meson and redundant photon. For experimental and simulated events selected using these requirements the fractions r_{MC} and r_{exp} of events satisfying standard selection criteria were calculated. The correction for the detection efficiency is determined as $\kappa = r_{exp}/r_{MC}$. It is equal to 0.956 ± 0.015 . The quoted error is statistical.

V. DETERMINATION OF THE BORN CROSS SECTION

The visible cross section σ_{vis} of the process under study, which is directly obtained from experimental data, is related to Born cross section σ_0 as:

$$\sigma_{vis}(\sqrt{s}) = \int_0^1 dz \cdot \sigma_0(\sqrt{s}(1-z)) \cdot F(z, s) \cdot \varepsilon(\sqrt{s}, z) \quad (6)$$

where $F(z, s)$ is a probability density function for the initial particles to emit photon carrying the fraction of energy $z\sqrt{s}$ [9], $\varepsilon(\sqrt{s}, z)$ is a detection efficiency as a function of \sqrt{s} and z . The experimental Born cross section is determined using following procedure. The measured visible cross section as a function of energy $\sigma_{vis,i} = N_i/IL_i$ (here N_i is a number of selected events after background subtraction for the i -th energy point, IL_i is an integrated luminosity for this point) is approximated by a function calculated using Eq. (6) with some model for the Born cross section. As a result of the approximation the parameters of this model are calculated together with the function $R(s) = \sigma_{vis}(s)/\sigma_0(s)$. Experimental values for the Born cross section are determined then according to the following equation:

$$\sigma_{0,i} = \frac{\sigma_{vis,i}}{R(s_i)}. \quad (7)$$

Model dependence of the result is estimated by variation of the Born cross section models.

The Born cross section of the process $e^+e^- \rightarrow K_S K_L$ was considered in a framework of the VDM:

$$\sigma_0(s) = \frac{12\pi}{s^{3/2}} \left| \sum_{V=\rho,\omega,\phi,\dots} \frac{\sqrt{\Gamma_{V \rightarrow K_S K_L}(s) \Gamma_{V \rightarrow ee} m_V^3} e^{i\theta_V}}{s - m_V^2 + im_V \Gamma_V(s)} \right|^2 \quad (8)$$

The ratios of partial widths and relative phases of ρ , ω , and ϕ mesons were taken according to SU(3) model:

$$\Gamma_{\rho \rightarrow K_S K_L}(s) = \Gamma_{\omega \rightarrow K_S K_L}(s) = 2\Gamma_{\phi \rightarrow K_S K_L}(s),$$

$$\theta_\rho = 0^\circ, \theta_\omega = 180^\circ, \theta_\phi = 180^\circ$$

The masses m_V and full widths Γ_V for the excitations of ρ , ω , ϕ were taken as in [11]. The approximation is done using program FIT [12]. The following models for the Born cross section were considered:

1. The process is described by four vector mesons ρ , ω , ϕ , $\rho(1450)$. The relative phase $\theta_{\rho(1450)} = 0^\circ$,
2. The process is described by four vector mesons ρ , ω , ϕ , $\phi(1680)$. The relative phase $\theta_{\phi(1680)} = 0^\circ$,
3. The process is described by four vector mesons ρ , ω , ϕ , $\rho(1700)$. The relative phase $\theta_{\rho(1700)} = 0^\circ$.

For the models described above the following χ^2 values were obtained: $\chi_1^2/ndf = 19.1/21$, $\chi_2^2/ndf = 18.9/21$, $\chi_3^2/ndf = 18.7/21$, respectively. All three models provide good approximation of the experimental data and can be used for the estimation of the Born cross section. Our final result is based on approximation by a second model. The cross section values are listed in Table I. Also shown in the table are the values of the detection efficiency and radiative corrections calculated as:

$$1 + \delta(s) = \frac{\int_0^1 dz \cdot \sigma_0(\sqrt{s}(1-z)) \cdot F(z, s)}{\sigma_0(s)} \quad (9)$$

$$\varepsilon(s) = \frac{\sigma_{vis}(s)}{\sigma_0(s) \cdot (1 + \delta(s))} \quad (10)$$

The function $R(s)$ introduced above is defined as $R(s) = \varepsilon(s)(1 + \delta(s))$.

VI. SYSTEMATIC ERRORS

The full systematic error on Born cross section of the process $e^+e^- \rightarrow K_S K_L$ includes several contributions: the integrated luminosity uncertainty, the uncertainty in the detection efficiency, the errors on the beam subtraction and radiative corrections estimations.

The error on integrated luminosity. The integrated luminosity at SND detector is determined using QED processes $e^+e^- \rightarrow e^+e^-$ and $e^+e^- \rightarrow \gamma\gamma$, for which the cross sections are known with a precision of better than 1%. As an estimate of the systematic error we take the difference between the luminosities obtained using these processes, which is about 2% almost independently of the beam energy.

The uncertainty of the detection efficiency The analysis of the systematic uncertainty of the detection efficiency was done using events from the ϕ -resonance energy region. The cross section of the process (1) was measured using events with four or more reconstructed photons. The events of this class contain four photons from the $K_S \rightarrow 2\pi^0$ decay and additional clusters from decays or nuclear interactions of K_L mesons or clusters from beam background. As it was described above the selection of the events of the process (1) is based on reconstruction of K_S meson. No constrains on additional photons were applied. Such approach minimizes the systematic error from the inaccuracy of the simulation of the nuclear interaction of K_L meson in the detector. Nevertheless, since it is not possible to

TABLE I: Born cross section of the process $e^+e^- \rightarrow K_S K_L$, measured by SND detector. N_{exp} — the number of selected events, $\sum N_{bkg}$ — the number of background events, ε_i — detection efficiency, $1 + \delta_i$ — radiative correction. The quoted errors are statistical and systematic, respectively

\sqrt{s} , GeV	IL, nb $^{-1}$	N_{exp}	$\sum N_{bkg}$	ε_i	$1 + \delta_i$	σ_0 , nb
1.04	69	245	3.0 ± 1.0	0.079	1.61	$27.3 \pm 1.8 \pm 0.8$
1.05	83	183	2.0 ± 0.8	0.078	1.81	$15.5 \pm 1.2 \pm 0.5$
1.06	274	421	2.5 ± 1.1	0.077	1.92	$10.3 \pm 0.5 \pm 0.3$
1.07	97	96	1.2 ± 0.6	0.076	1.78	$7.2 \pm 0.8 \pm 0.2$
1.08	572	420	6.2 ± 1.3	0.075	1.49	$6.4 \pm 0.3 \pm 0.2$
1.09	94	48	0.9 ± 0.4	0.074	1.30	$5.2 \pm 0.8 \pm 0.2$
1.10	436	158	4.8 ± 0.9	0.073	1.20	$4.0 \pm 0.3 \pm 0.1$
1.11	88	21	1.3 ± 0.4	0.072	1.13	$2.75 \pm 0.65 \pm 0.08$
1.12 – 1.13	420	97	5.6 ± 1.0	0.071	1.09	$2.81 \pm 0.30 \pm 0.09$
1.14 – 1.15	358	61	3.6 ± 0.7	0.069	1.05	$2.22 \pm 0.30 \pm 0.07$
1.16	316	40	2.3 ± 0.5	0.067	1.02	$1.74 \pm 0.29 \pm 0.05$
1.18 – 1.19	587	44	4.3 ± 0.8	0.065	1.00	$1.04 \pm 0.18 \pm 0.03$
1.20 – 1.21	569	32	3.7 ± 0.7	0.063	0.99	$0.80 \pm 0.16 \pm 0.03$
1.22 – 1.23	465	25	3.8 ± 0.8	0.060	0.99	$0.77 \pm 0.18 \pm 0.02$
1.24 – 1.25	562	22	2.2 ± 0.5	0.058	0.98	$0.62 \pm 0.15 \pm 0.02$
1.26 – 1.27	397	16	1.6 ± 0.4	0.056	0.98	$0.66^{+0.24}_{-0.18} \pm 0.02$
1.28 – 1.29	492	20	2.4 ± 0.6	0.054	0.97	$0.68^{+0.22}_{-0.17} \pm 0.02$
1.30 – 1.31	459	11	1.0 ± 0.2	0.052	0.97	$0.43^{+0.19}_{-0.14} \pm 0.01$
1.32 – 1.33	516	3	2.1 ± 0.5	0.050	0.97	$0.04^{+0.12}_{-0.07} \pm 0.01$
1.34 – 1.35	676	13	2.7 ± 0.6	0.048	0.97	$0.33^{+0.15}_{-0.11} \pm 0.01$
1.36	606	11	3.1 ± 0.7	0.047	0.96	$0.29^{+0.16}_{-0.12} \pm 0.01$
1.37 – 1.38	722	11	2.2 ± 0.5	0.045	0.96	$0.28^{+0.14}_{-0.11} \pm 0.01$

distinguish the clusters from the K_S -meson decays from those from those produced by K_L meson or beam background, these additional clusters give rise to a combinatorial background where lost or misreconstructed photons from K_S decay are replaced by clusters produced by K_L or beam background. The more such clusters, the larger number of misreconstructed K_S mesons. This effect leads to an uncertainty of the detection efficiency due to inaccuracy of simulation of the K_L -meson interactions in the detector material. This includes not only the inaccuracy of the total cross section of the nuclear interaction of K_L meson, but also the inaccuracy of the number of clusters and energy depositions in the calorimeter counters.

The total systematic error on detection efficiency is a sum of the uncertainty for the “pure” K_S meson and uncertainty of the combinatorial background increased by inaccuracy of the simulation of the nuclear interaction of K_L meson in the detector.

The uncertainty of the simulation of the “pure” K_S meson was studied using events, in which the K_L meson is reconstructed as a single photon. The selection criteria for these events are described in section IV. It was found that corresponding correction to the efficiency estimated by simulation is equal to 0.956 ± 0.015 . This correction accounts for the differences in distributions in χ^2 (3%) and photon quality parameter (2%).

The systematic error on combinatorial background and nuclear interaction of K_L mesons was estimated as a difference between the detection efficiency values obtained by two ways. The first, standard, way is to estimate detection efficiency ε_{MC} as the ratio of the numbers of selected signal events to the total number of simulated events. The second way is to first estimate the detection efficiencies for the subsets of simulated events with fixed numbers of reconstructed photons and then to average obtained values according to relative weights observed in data. The ratio of the efficiencies obtained in this way is $\varepsilon_{MC}^*/\varepsilon_{MC} = 0.991 \pm 0.007$. Corresponding systematic uncertainty is equal to 1%.

Another source of systematic uncertainty is the difference in energy and angular resolutions for photons between data and simulation. This difference affects the resolution in recoil mass of the reconstructed K_S meson shown in Fig. 3 and in the slope of the dependence of the detection efficiency of the process (1) on E_γ , shown in Fig. 5. To evaluate this contribution into the systematic error we varied the slope of the efficiency dependence on E_γ within limits corresponding to observed 2% difference in K_S recoil mass resolution in data and simulation on ϕ resonance.

The total systematic error on detection efficiency changes from 2.1% to 2.5% with the

TABLE II: Systematic uncertainties of the measured Born cross section of the process $e^+e^- \rightarrow K_S K_L$.

Source	1.02 — 1.40 GeV
Integrated luminosity	2%
Detection efficiency	2.1—2.5%
Background subtraction	0.1—2.9%
Model dependence	0.5 — 3.0%
Total	2.9 — 5.3%

energy in the range 1.04 – 1.4 GeV.

Background subtraction. As it was mentioned above, the contributions of background processes 2 and 3 well agree with with estimations based on simulation. Therefore the extraction of the Born cross section from the experimental data the estimated by simulation number of background events of these processes was subtracted. The beam background was estimated from the $\chi^2_{K_S \rightarrow 2\pi^0}$ distribution of the experimental events. The systematic error on the background subtraction varies from 0.1% to 2.9% for the energy range from 1.04 up to 1.40 GeV. The statistical error on the background subtraction is included into the quoted statistical error of the measured cross section.

Accuracy of the radiative corrections This systematic error includes the theoretical uncertainty of the radiative correction calculation, which does not exceed 0.1% [9], and model dependence, related to the choice of the model describing the energy dependence of the cross section being measured. As an error estimate the difference between results obtained with the different choices of the approximation function described in section V. The systematic error from radiative correction uncertainty varies between 0.5% and 3.0% in the energy range from 1.04 to 1.40 GeV.

The total systematic errors are listed in Table II.

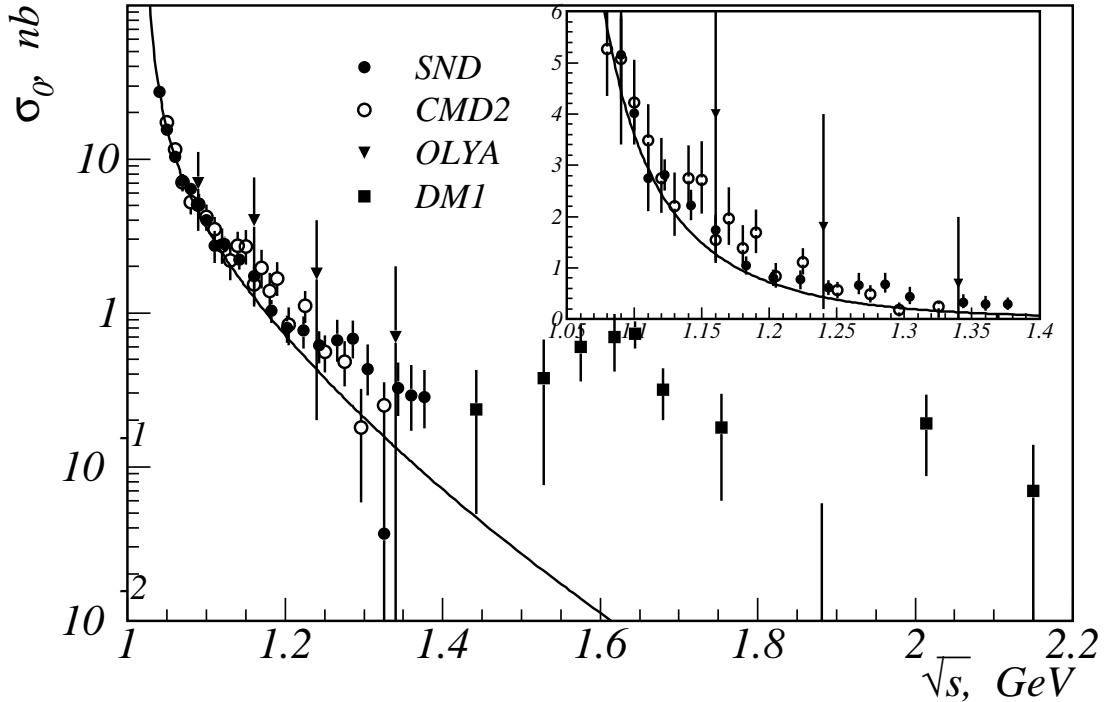


FIG. 6: Born cross section of the process $e^+e^- \rightarrow K_S K_L$. Dots with error bars represent results obtained by SND(this work), CMD-2[5], OLYA[4] and DM1[3] detectors. Solid line represents the cross section calculated using VMD with $\rho(770)$, $\omega(783)$, $\phi(1020)$ taken into account.

VII. DISCUSSION

In Fig. 6 the cross sections measured in this work and previous measurements by OLYA, CMD-2, and DM1 detectors are shown. The results are in good agreement with ones obtained by CMD-2 and OLYA in the same energy region.

The measured cross section of the process $e^+e^- \rightarrow K_S K_L$ significantly exceeds one predicted by VMD model with only $\rho(770)$, $\omega(783)$, and $\phi(1020)$ resonances considered within SU(3) model. The curve corresponding to this prediction is shown in Fig 6. The measured cross section significantly exceeds this VMD estimation starting from the energy about 1.2 GeV. This excess can be described by contributions from higher mass states ρ' , ω' , and ϕ' , but for the determination of the parameters of these states the data in wider energy range and for other decay modes are needed.

This work was partially supported by the RFFI grants 05-02-16250-a, 04-02-16181-a,

04-02-16184-a and the Sci.School-905.2006.2.

- [1] M. N. Achasov *et al.*, Phys. Rev. D, **63** (2001) 072002,
- [2] R. R. Akhmetshin *et al.*, Nucl. Phys. Proc. Suppl. **131** (2004) 3,
- [3] F. Mané *et al.*, Phys. Lett. B, **99** (1981) 261,
- [4] P. M. Ivanov *et al.*, Pisma v JETP, **36** (1982) 91 (in Russian),
- [5] R. R. Akhmetshin *et al.*, Phys. Lett. B **551** (2003) 27,
- [6] M. N. Achasov *et al.*, Nucl. Instr. and Meth. A **449** (2000) 125,
- [7] A. V. Bozhenok, V. N. Ivanchenko, Z. K. Silagadze, Nucl. Instr. and Meth., A **379** (1996) 507,
- [8] M. N. Achasov, K. I. Beloborodov, A. V. Berdyugin *et al.*, Phys. Lett. B **486** (2000) 29,
- [9] E. A. Kuraev, V. S. Fadin, Sov. J. Nucl. Phys., **41** (1985) 466,
- [10] G. Bonneau, F. Martin, Nucl. Phys. B **27** (1971) 381,
- [11] S. Eidelman *et al.*, Phys. Lett. B, **582** (2004) 1,
- [12] A. V. Bozhenok, D. A. Bukin, V. N. Ivanchenko *et al.*, Preprint IYaF 99-103, Novosibirsk, 1999.